

ROSAT all-sky survey observations of Pop II field binaries: X-ray activity of old, metal-poor stellar coronae

R. Ottmann¹, T.A. Fleming², and L. Pasquini³

¹ Max-Planck-Institut für extraterrestrische Physik, D-85748 Garching, Germany

² Steward Observatory, University of Arizona, Tucson, AZ 85721, USA

³ European Southern Observatory, Casilla 19001, Santiago 19, Chile

Received 22 April 1996 / Accepted 24 July 1996

Abstract. This study represents the first X-ray observations of an extended sample of Pop II field binaries, aimed at investigating the properties of old, metal-poor stellar coronae. Analysing X-ray observations from the ROSAT all-sky survey, we detected only 13 (out of 86) Pop II systems (15% detection rate). The X-ray luminosity function, taking into account both detections and upper limits, has its median at $\log L_x \leq 28.1 \text{ erg s}^{-1}$, indicating a low average X-ray luminosity, with a high-luminosity tail at $\log L_x \sim 29 - 31 \text{ erg s}^{-1}$. The only extreme metal-poor system detected is HD 89499. Thus, the detection rate of extreme Pop II systems is lower than of intermediate Pop II, possibly indicating extreme Pop II to be typically less luminous. The X-ray luminosity is not very well correlated with orbital period; long-period Pop II binaries may have high X-ray luminosities and, surprisingly, short-period systems are not *per se* strong X-ray emitters. For a subsample of emission-line Pop II binaries, i.e. the halo component analogs to the RS CVn binaries, the median X-ray luminosity is at least one order of magnitude lower than for the RS CVns. The lower activity levels of the Pop II systems may be caused in part by the presence of fewer evolved stars in the sample and lower metallicity. The extremely old age of Pop II binaries may also give rise to the unexpectedly low X-ray luminosities of some systems (e.g., CD-481741, BD+53080).

Key words: stars: activity – stars: binaries: close – stars: coronae – stars: Population II – X-rays: stars

1. Introduction

So far, the phenomenon of coronal activity has been studied almost exclusively for stars belonging to the Galactic disk. These are metal-rich objects with low space-velocities, which have been formed during later stages of Galactic evolution. Hence,

our present knowledge about stellar coronae refers to high-metallicity, relatively young systems. The reason for this concentration on Pop I objects is that the majority of nearby stars belong to the disk component. Stars of the Galactic halo have weak metallic lines and large space velocities. They have formed during the collapse of the Galaxy, long before the disk configuration has settled. Halo stars differ significantly from disk objects with respect to metallicity, age, and, presumably, in the nature of their coronae. The halo component consists of globular clusters and field stars. As globular clusters are rather distant, field stars are far better suited to study the coronae of Pop II objects.

Extremely old single stars are expected to be slow rotators and, hence, weak X-ray emitters, as a result of the permanent loss of angular momentum due to magnetic braking. Extremely old binary systems can still possess high rotation rates due to their synchronous rotation. If Pop II coronal activity, similar to that of Pop I systems, essentially depends on the rotation rate, Pop II binaries may be vigorous X-ray emitters. Therefore, one can study the effect of metallicity and age on the activity of stellar coronae by comparing the X-ray luminosities of Pop II with those of Pop I binaries. Since the bulk of coronal radiation is emitted in lines from elements such as Fe, it is clearly a function of metallicity. The effect of stellar age on main-sequence, short-period binary systems is not yet clear; it might be a decrease in the production rate of magnetic flux, or a dynamical effect due to the longer times of tidal interaction.

The survey of about 900 proper motion stars by Carney and Latham (1987) – together with a similar program by Sandage and Fouts (1987) – provided the first extended photometric database of halo field stars. For part of this sample, Laird et al. (1988) determined photometric reddenings and parallaxes, and spectroscopic metallicities. Further, Latham et al. (1988, 1992) obtained orbits for 80 spectroscopic binaries of the sample by radial-velocity measurements. This proper-motion survey provided the basis for a number of subsequent studies, aimed at investigating the atmospheric activity of Pop II field binaries. Pasquini et al. (1991) found evidence for strong chromospheric activity in 4 short-period Pop II binaries, from which

Send offprint requests to: R. Ottmann, MPE address

one (HD 85091) was detected by ROSAT as the first Pop II coronal source. Next, Pasquini and Lindgren (1994) analyzed Ca II and H α observations of a sample of 27 Pop II binaries, and found systems with periods less than 10 days to possess active chromospheres. Finally, while modelling the spectra of 16 metal-poor binaries, Spite et al. (1994) found about half of them to be slightly evolved. While these studies are concerned mainly with the optical properties of Pop II binaries, their X-ray properties are largely unknown. So far, X-ray studies have been performed only for two Pop II binaries: Besides the X-ray detection of HD 85091, only the extremely metal-poor system HD 89499 (Gehren 1982, Hartmann and Gehren 1988) has been studied by ASCA and ROSAT (Fleming 1996). With regard to the wealth of X-ray data available for Pop I binaries, it is clear that further X-ray observations of Pop II binaries are required to enable a reliable comparison between halo and disk binaries.

The ROSAT all-sky survey is ideally suited for providing X-ray data for a large sample of Pop II binaries, because it yields a complete and flux-limited coverage of the entire sky. The ROSAT survey data allow the determination of X-ray luminosities and hardness ratios for each Pop II binary. From the X-ray parameters of the individual objects, mean X-ray properties, characteristic for the class of Pop II binaries, can be derived by means of statistical methods. By a comparison between the X-ray properties of halo and disk binaries, conclusions about the effects of metallicity and age on the coronal activity can be derived.

In Sect. 2, we define our input sample of Pop II binaries and compile its optical properties. In Sect. 3, we describe the X-ray observations and the applied source detection technique. Sect. 4 contains the results of our X-ray analysis. In Sect. 5, the X-ray luminosity function of the Pop II binaries is computed. In Sect. 6, we investigate which stellar properties determine coronal activity in Pop II binaries. Finally, a summary and discussion on the effects of metallicity and age is given in Sect. 7.

2. The input optical sample

Up to now, the number of Pop II field binaries with known orbits has been rather limited compared to the wealth of orbital solutions available for Pop I binaries. Orbital parameters have been published so far only for about 90 systems. In Table 1, we have compiled a list of 86 Pop II field binaries of spectral types F to K, which forms our optically selected input sample. The main source for our compilation is the radial-velocity study of 80 spectroscopic binaries by Latham et al. (1988, 1992), which come from the survey of proper-motion stars by Carney and Latham (1987). From the sample of Latham et al. (1988, 1992), we selected 72 metal-poor systems with $[m/H] < -0.4$. We added to this primary list another 14 systems which have been the subject of detailed investigations by Peterson et al. (1980), Mayor and Turon (1982), Lindgren et al. (1987), Ardeberg and Lindgren (1991), and Lindgren and Ardeberg (1995). Our sample stars are located mainly in the northern sky.

In Table 1, the optical properties of the Pop II binaries are listed. The photometry V , $B - V$ and the orbital parameters

P_{orb} , e are taken mainly from Latham et al. (1988, 1992), as indicated by the first entry in the reference column. The orbital periods range from 1.8 to 2000 d. For HD 106516, two different orbital solutions are reported: Latham et al. (1992) found a very long period of $P_{orb} = 853.2$ d, while Abt and Willmarth (1987) suggested a shorter period of $P_{orb} = 23.1$ d. Our finding, that HD 106516 possesses a quite active X-ray corona (cf. Sect. 4), seems to argue in favour for the shorter period. The metallicities $[m/H]$ are taken, if available, from Spite et al. (1994), otherwise from Laird et al. (1988), as indicated by the second entry in the reference column. The metallicities range from -0.4 to -2.9 , showing that the sample contains both intermediate and extreme Pop II stars. The surface gravities g are taken from the high-quality spectra of Spite et al. (1994). The chromospheric indices A_k are adopted from Pasquini and Lindgren (1994) or were obtained by us at the McMath telescope (Kitt Peak, AZ), as indicated by the fourth entry in the reference column. The A_k values measure the amount of flux between the K_1 points of the CaII K line, normalised to the continuum flux at 3950Å. Thus, A_k is a measure of the chromospheric activity of the active star within the binary system, normalised to the continuum flux of the primary.

As a coronal activity measure, we will preferentially use the integral X-ray luminosity of the binary system (cf. Sect. 6). To obtain accurate values for the X-ray luminosities, a careful determination of the stellar distances d is essential. The distances quoted in Table 1 are determined as follows:

(i) Since most of our stars are more distant than 50 pc, the most reliable method to derive stellar distances is by means of spectroscopic gravities, which are available for 18 stars in our sample. For the 9 evolved stars with surface gravities $\log g < 4.0$, the distances are estimated from theoretical evolutionary tracks calculated by Van den Berg and Bell (1985) for low metallicity stars. We consider the tracks with a He fraction $Y = 0.2$, which is close to the primordial He abundance of presumably $Y = 0.23 - 0.24$ (Boesgaard and Steigman, 1985), and a metal fraction Z according to the star's metallicity. The values of $\log g$ and $B - V$ are used to determine the position of the star along the appropriate track. For larger distances and/or low galactic latitudes the effect of reddening is taken into account. For the 9 dwarf stars with $\log g \geq 4.0$, the relation between absolute magnitude M_V and $B - V$ derived by Laird et al. (1988) for metal-poor dwarfs is applicable, so we use this relation to estimate distances. Two of the dwarf stars, HD 111980 and BD -00 4234, are not contained in the sample of Laird et al. (1988); their distances are also estimated from evolutionary tracks. The thus derived spectroscopic distances are expected to be rather reliable ($\sigma_d/d \sim 0.2$ assumed).

(ii) Trigonometric parallaxes, as measured from the ground, have recently been found to be reliable only for distances less than about 50 pc (e.g., Grenon 1995). Therefore, trigonometric distances d_t are given only if there are no gravity measurements. Thus, trigonometric distances are quoted for 16 stars. About half of these parallaxes have acceptable statistical errors $\sigma_\pi/\pi_t \leq 0.5$. The remaining trigonometric distances have sta-

Table 1. Optical Properties of the Pop II Field Binaries.

Name	V	B-V	P_{orb} (d)	e	[m/H]	log g	d (pc)	Δd_t (pc)	A_k	References	Notes
HD 111980	8.38	0.54	12.43	0.0	-0.9	4.0	70	[45,166]	0.093	MT,S,vB,Pa	
CD -48 1741	10.68	0.51	7.56	0.0	-1.4	4.0	85	[30,170]	0.150	Li,S,Li,Pa	
HD 149414	9.58	0.74	133.29	0.273	-1.4	3.5	160	[18,26]	0.086	MT,S,vB,Pa	
BD -3 2525	9.66	0.48	113.55	0.464	-2.29	-	166	[71, ∞]	-	L,La,J,-	DLSB
BD +13 3683	10.57	0.67	40.26	0.365	-2.3	4.0	57	-	0.069	L, S,La,Pa	
BD +13 13	8.59	0.81	1.84	0.007	-0.4	3.0	150	-	0.670	L, S,vB,Pa	
HD 3266	7.98	0.67	36.00	0.450	-1.16	-	37	[30,48]	0.090	L, La,J ,Mc	vc
G 103-50	12.07	0.86	85.91	0.17	-2.40	-	-	-	-	L, L,-,-	DLSB
G 88-10	11.87	0.44	20.63	0.300	-2.7	4.0	181	-	0.106	L, S,La,Pa	
G 89-14	10.40	0.46	190.31	0.401	-1.88	-	97	-	-	L, La,La,-	
HD 64606	7.43	0.73	446.65	0.357	-1.0	3.8	43	[17,28]	0.060	L, S,vB,Pa	
HD 85091	7.62	0.60	3.39	0.002	-0.5	3.5	73	[43,111]	0.440	L, S,vB,Pa	
BD +30 2130	9.29	0.62	6.57	0.004	-0.4	3.3	160	-	0.210	L, S,vB,Pa	
BD +21 2321	11.51	0.64	80.31	0.368	-0.9	4.0	137	-	0.086	L, S,La,Pa	
HD 108754	9.03	0.70	25.94	0.158	-0.83	-	22	[17,30]	0.073	L, La,J,Pa	
G 206-34	11.39	0.43	32.39	0.497	-2.9	4.0	162	-	-	L, S,La,-	
BD +10 3711	10.54	0.54	386.92	0.204	-1.57	-	103	-	-	L, La,La,-	DLSB
BD +17 4708	9.47	0.44	219.38	0.337	-1.5	3.3	210	[45,125]	0.108	L, S,vB,Pa	
HD 89499	8.66	0.72	5.57	0.0	-2.1	2.0	220	[17,50]	0.330	AL,S,vB,Pa	
HD 224621	9.59	?	?	?	?	-	-	-	-	?	
HD 6308	8.8	?	?	?	?	-	-	-	-	?	
HD 6286	8.23	0.96	35.7	0.02	-1.4	-	55	-	1.180	LA,LA,He,Pa	
HD 24202	8.81	0.61	18.8	0.25	-1.1	-	-	-	0.121	LA,LA,-,Pa	
HD 29907	9.86	0.64	29.9	0.41	-1.7	-	333	[90, ∞]	0.074	LA,LA,J ,Pa	
HD 30229	9.41	0.66	139.6	0.01	-2.5	-	-	-	0.065	LA,LA,-,Pa	
HD 274680	10.28	0.46	?	?	?	-	-	-	-	?	
BD +5 3080	9.14	0.83	9.94	0.069	-0.7	4.0	27	-	0.430	L,S,La,Pa	
HD 175706	8.6	?	?	?	?	-	-	-	-	?	
CD -37 14010	9.77	0.99	65.5	0.0	-2.6	-	-	-	0.065	LA,LA,-,Pa	
BD -00 4234	9.81	0.95	3.76	0.018	-0.7	4.0	30	[38,160]	1.000	P,S,vB,Pa	
HD 245	8.37	0.65	71.5	0.216	-1.07	-	91	[50,500]	-	L, La,J,-	
HD 20507	6.93	0.45	26.77	0.142	-0.96	-	125	[55, ∞]	-	L,La,J,-	
HD 23439B	8.78	0.88	48.67	0.673	-1.02	-	25	-	-	L, La,La,-	
G 87-47	10.34	0.66	13.73	0.464	-1.41	-	59	-	-	L, La,La,-	
G 236-38	12.82	0.78	26.70	0.26	-1.41	-	154	-	-	L, La,La,-	DLSB
G 176-27	11.29	0.83	11.73	0.023	-2.12	-	63	-	-	L, La,La,-	DLSB
BD +36 2193	9.89	0.67	7.15	0.008	-0.64	-	74	-	-	L, La,La,-	
G 178-56	11.90	0.70	249.68	0.400	-1.15	-	126	-	-	L, La,La,-	
G 262-14	11.47	0.77	81.19	0.424	-0.96	-	93	-	-	L, La,La,-	
HD 195987	7.06	0.79	57.32	0.316	-0.83	-	20	[18,23]	0.18	L, La,J,Mc	
G 230-45	11.43	0.80	398.9	0.200	-0.84	-	89	-	-	L, La,La,-	
HD 200077	6.59	0.55	112.55	0.686	-0.78	-	59	[45,83]	-	L, La,J,-	
G 215-47	12.17	0.56	318.41	0.317	-1.26	-	219	-	-	L, La,La,-	
G 190-10	11.22	0.61	30.15	0.225	-1.96	-	91	-	-	L, La,La,-	
G 217-2	12.01	0.64	49.34	0.294	-0.74	-	220	-	-	L, La,La,-	
G 171-23	13.24	0.66	153.99	0.027	-0.96	-	306	-	-	L, La,La,-	
BD +13 308	10.94	0.89	20.71	0.398	-0.59	-	-	-	-	L, L,-,-	
BD +15 150	10.66	0.54	346.38	0.372	-1.77	-	-	-	-	L, L,-,-	$M_2 > M_1$
BD +47 451	11.00	0.70	1012.	0.452	-1.13	-	93	-	-	L, La,La,-	
BD +48 476	10.13	0.51	62.97	0.156	-1.56	-	-	-	-	L, L,-,-	DLSB
BD +27 335A	9.99	0.79	207.8	0.212	-0.50	-	-	-	-	L, L,-,-	cpmp
BD +27 335B	10.55	0.88	88.18	0.156	-0.47	-	-	-	-	L, L,-,-	cpmp
BD +43 538	10.18	0.52	227.3	0.304	-0.60	-	-	-	-	L, L,-,-	
HD 17841	8.38	0.79	28.96	0.292	-0.76	-	-	-	-	L, L,-,-	DLSB
HD 20039	8.89	0.75	114.38	0.381	-1.13	-	143	[59, ∞]	-	L,La,J,-	DLSB

Table 1. (continued)

Name	V	B-V	P_{orb} (d)	e	[m/H]	log g	d (pc)	Δd_t (pc)	A_k	References	Notes
HD 22694	8.19	0.83	8.65	0.394	-1.02	-	20	-	0.560	L, L,L ,Pa	DLSB; cpmp
HD 30455	6.95	0.64	45.43	0.338	-0.67	-	83	[50,250]	-	L, L,J,-	
BD +72 245	9.89	0.79	7.53	0.011	-0.48	-	59	[37,143]	-	L, L,J,-	
BD +4 865	10.58	0.79	8.66	0.012	-0.79	-	146	-	-	L, L,La,-	
G 86-40	11.83	0.59	108.48	0.256	-2.38	-	146	-	-	L, La,La,-	DLSB
G 99-52	12.76	0.72	560.0	0.199	-1.54	-	170	-	-	L, La,La,-	
BD +38 1670	9.46	0.64	85.05	0.239	-1.14	-	55	-	0.16	L, L,SF,Mc	
BD +46 1314	9.43	0.60	41.97	0.410	-0.96	-	-	-	-	L, L,-,-	
BD +20 2030	11.20	0.38	60.59	0.462	-2.68	-	165	-	-	L, L,L,-	
BD +52 1397	9.46	0.59	16.93	0.016	-0.63	-	-	-	-	L, L,-,-	
BD +0 2627	10.24	0.67	1259.	0.30	-0.49	-	93	-	-	L, La,La,-	
G 253-41	11.74	0.50	237.63	0.393	-1.45	-	182	-	-	L, La,La,-	
G 253-44	11.99	0.82	19.39	0.520	-1.01	-	117	-	-	L, La,La,-	
G 176-46	12.59	0.80	10.44	0.054	-1.67	-	127	-	-	L, La,La,-	DLSB; t
HD 106516	6.12	0.45	23.1	0.0	-0.7	4.2	19	[30,45]	-	AW, S,La,-	$P_{orb} : 853(L)$
BD +28 2137	10.90	0.41	60.18	0.552	-2.2	3.5	500	-	-	L, S,vB,-	
BD +21 2442	8.98	0.80	31.02	0.561	-0.90	-	30	-	0.32	L, La,La,Mc	DLSB
G 62-40	13.55	0.76	95.45	0.462	-1.97	-	201	-	-	L, La,La,-	
G 178-27	11.24	0.43	80.82	0.437	-2.08	-	-	-	-	L, L,-,-	
G 66-59	13.20	0.64	10.74	0.001	-2.61	-	189	-	-	L, La,La,-	DLSB
HD 149162	8.84	0.88	226.3	0.324	-1.39	-	27	[22,33]	-	L, L,J,-	$M_2 > M_1$
HD 157948	8.10	0.76	448.87	0.150	-1.26	-	19	-	-	L, La,La,-	DLSB; vc
G 183-9	11.87	0.53	6.20	0.014	-1.63	-	-	-	-	L, L,-,-	
G 262-32	10.73	0.82	52.91	0.445	-0.95	-	61	-	-	L, La,La,-	
HD 200580	7.34	0.54	377.82	0.086	-1.00	-	333	[125, ∞]	-	L,La,J,-	t
BD +11 4725	9.55	0.65	1680.	0.168	-0.88	-	54	-	-	L, La,La,-	
G 18-54	10.70	0.48	491.5	0.183	-1.67	-	-	-	-	L, L,-,-	
HD 218568	9.27	0.66	1148.	0.233	-0.79	-	53	-	-	L, La,La,-	
BD +38 4955	11.04	0.66	183.85	0.771	-2.5	-	19	[9, ∞]	-	L, S,J,-	
G 29-71	11.34	0.53	2269.	0.202	-2.4	3.5	430	-	-	L, S,vB,-	
BD +33 4813	8.50	0.65	956.	0.476	-0.57	-	-	-	-	L, L,-,-	

Columns: (1) Stellar identification, (2) apparent magnitude, (3) colour, (4) Orbital period, (5) eccentricity, (6) metallicity, (7) gravity, (8) distance, (9) trigonometric distance interval (reference: J), except for HD 89499 (reference: AL), (10) chromospheric index, (11) references: first: V, B-V, P_{orb} , e, second: [m/H], third: d , fourth: A_k (11) Notes.

References: L: Latham et al. (1988), (1992); AL: Ardeberg and Lindgren (1991); P: Peterson et al. (1980); Li: Lindgren et al. (1987); MT: Mayor and Turon (1982); LA: Lindgren and Ardeberg (1995); S: Spite et al.(1994); La: Laird et al. (1988); AW: Abt and Willmarth (1987); He: Heard (1956); J:Jenkins (1952), (1963); Sandage and Fouts (1987); vB: Van den Berg and Bell (1985); Pa: Pasquini and Lindgren (1994); Mc: taken at McMath telescope.

Abbreviations: M_1 , M_2 : primary and secondary masses (in M_\odot); vc: visual companion; cpmp: common proper motion pair; t=triple system; DLSB=double line spectroscopic binary

tistical errors greater than 50%, and correspondingly a large uncertainty range.

(iii) For the 37 stars in our sample for which both the surface gravity and the trigonometric parallax are unknown, we use again the photometric parallaxes determined by Laird et al. (1988). If the stars are dwarfs, then the photometric distances are reliable ($\sigma_d/d \sim 0.2$ assumed). However, the fraction of subgiants and giants within the entire proper-motion sample is estimated to be about 10% (Laird et al., 1988), and is even higher within our binary sub-sample, as is indicated by the log g - measurements. As a consequence, at least 10% of the photo-

metric distances are strongly underestimated. This systematic error cannot be taken into account.

In total, distances are quoted for 65 out of the 86 sample stars. The reference for the distances is indicated by the third entry in the reference column. For HD 149414 and HD 89499, the spectroscopic distances are far above the trigonometric distance ranges (cf. column ' Δd_t ' of Table 1), indicating that the trigonometric distances of these stars are probably wrong. In the case of HD 89499, the spectroscopic distance is one order of magnitude larger than its trigonometric value. The large value of the hydrogen column density of $N_H = 4 \cdot 10^{20} \text{ cm}^{-2}$, de-

rived from ROSAT and ASCA X-ray spectra (Fleming and Tagliaferri 1996), would seem to suggest the larger distance.

Because our sample is optically selected, it is not *a priori* biased towards X-ray luminous Pop II binaries. However, our sample is not volume-limited and may therefore contain a slightly higher fraction of subgiants and giants than a complete (i.e., volume-limited) sample.

3. X-ray data analysis

The all-sky survey performed by the Röntgensatellit (ROSAT; Trümper 1983) provides an excellent opportunity to obtain X-ray observations for the entire Pop II sample. The ROSAT all-sky survey (RASS) was performed with the Position Sensitive Proportional Counter (PSPC; Pfeffermann et al., 1987) between July 1990 and January 1991. Parts of the sky missed during this period were observed in February and August 1991. The PSPC has an energy range of 0.1 – 2.4 keV, and a spectral resolution $\Delta E/E \sim 0.42$ at 1 keV. In the survey mode, the sky was scanned along great circles perpendicular to the ecliptic plane, with the scan period being synchronized to the orbital period of 96 min. In the 2° field of view of the PSPC, an X-ray source was visible for ≤ 30 s per scan. The visibility interval for each Pop II binary was determined by its ecliptic latitude, but lasted for at least 2 d. The resulting exposure times amounted to 300 – 1700 s, with a mean value of 770 s.

For each Pop II binary in our sample, we extracted $1^\circ \times 1^\circ$ regions of the sky, centered at the respective optical position. All source searches were conducted in three energy bands: Total: PSPC channels 8 – 240 (0.1 – 2.4 keV), Soft: 8 – 41 (0.1 – 0.28 keV), and Hard: 52 – 201 (0.5 – 2.0 keV). The source detection was performed by means of a maximum likelihood (ML) algorithm (cf. Cruddace et al., 1989). This algorithm calculates the probability p that the observed photon distribution matches the distribution derived from the theoretical point-spread function. The source parameters (counts, position, extent) are varied to maximize the likelihood $l \equiv -\ln(1 - p)$. All of the source detection analysis was performed by using the EXSAS software (Zimmermann et al. 1994).

For each of the 86 RASS data sets, the following source detection technique is applied to the X-ray images of the total, soft, and hard bandpasses:

- (i) All obvious sources are found using the LDETECT source detection algorithm (Cruddace et al., 1989). These sources are extracted from the X-ray image. The remaining image is then fitted by a spline function to give a smoothed background image.
- (ii) The source detection is performed with an ML algorithm. The search is started from the optical position. Since we expect differences between the optical and X-ray positions due to errors in the RASS attitude solution, the position is taken as free parameter. The X-ray peak closest to the optical position is found. The source counts within a $5'$ radius around the X-ray position are determined. The $5'$ extraction radius will contain 98% of the total source counts.
- (iii) A detection threshold of $ML = 7.0$, corresponding to an existence probability $p = 99.91\%$, was chosen. Therefore, we

would expect 0.08 false detections (i.e., practically none) within our 86 trials. Sources with $ML \geq 7.0$ are considered as detections. For sources with $ML < 7.0$, upper limits on the source counts are computed. The upper limit gives the number of counts within the extraction radius needed above the background to detect a source with a certain confidence level. We adopted a confidence level of 99.91% (i.e., 3σ).

For the minority of times during the RASS when the attitude was calculated from the gyros instead of the star trackers, the attitude solution was not correct and the detected photons had an incorrect position, about $10'$ off in ecliptic latitude. As a consequence, some RASS sources were shifted as a whole or split into two images. We did not find evidence for this positional offset in the X-ray images of our Pop II stars, although it is possible that we obtain only upper limits for sources which actually would have been detections. However, since only a few percent of the RASS sources are estimated to suffer from this attitude problem (Voges 1995), we should miss at most one detection if any.

4. X-ray detections and upper limits

The results of our source detection analysis for the total PSPC bandpass are given in Table 2. For each star, the Maximum Likelihood value for X-ray source existence and the difference between X-ray and optical position are listed. For the X-ray detections, the total PSPC count rate and its 1σ error, the hardness ratio and its 1σ error, and the derived X-ray luminosity based upon the distance given in Table 1 are provided. For the non-detected stars, the upper limits (corresponding to 99.91% confidence) on count rate and X-ray luminosity are indicated. At the chosen detection threshold ($ML = 7.0$), there are 15 X-ray sources detected in the total PSPC band (cf. Table 2). In addition, 1 source was detected only in the soft band, and 2 sources were detected only in the hard band.

Next, we have to estimate the maximum positional offset between the optical and X-ray positions to be used for identification. The cumulative distribution Φ of the radial positional offsets Δ may be approximated by a Gaussian distribution, $\Phi(\Delta) \propto 1 - \exp(-\frac{\Delta^2}{2\sigma^2})$, with σ denoting the characteristic radial positional error. The X-ray position as determined by the ML algorithm has a radial positional error of $\sigma_X \sim 15''$. Out of the 18 X-ray detections, 12 detections have an optical to X-ray positional offset $\Delta \leq 30''$, despite the fact that the optical position is not corrected for proper motion. As the mean density of RASS sources amounts to about 10^{-7} arcsec $^{-2}$, the number of background sources within a circle of $30''$ radius is only $3 \cdot 10^{-4}$. Thus, these 12 X-ray detections (containing the soft band detection) are true identifications. Furthermore, for HD 89499, which has a large proper motion, the positional offset is reduced to $\Delta = 30''$ if the correction for proper motion is applied. This gives us 13 true identifications. The remaining two detections in the total bandpass, G 103-50 and BD +13 308, are probably not true identifications, because their positional offsets (cf. Table 2) are too large to be explained either by proper motion or statistical fluctuations of the X-ray positional error.

Table 2. The Pop II Binaries in the RASS (total PSPC bandpass).

Name	Exposure (s)	ML	Δ ($''$)	count rate (s^{-1})	HR	L_X (erg s^{-1})	Notes
HD 111980	459	0.0	106	< 0.0151		$< 7.1e + 28$	
CD -48 1741	1321	0.5	69	< 0.0051		$< 3.6e + 28$	
HD 149414	822	2.5	111	< 0.0102		$< 2.5e + 29$	
BD -3 2525	597	3.0	120	< 0.0238		$< 6.3e + 29$	
BD +13 3683	781	0.3	239	< 0.0106		$< 3.3e + 28$	
BD +13 13	450	817.8	5	0.9995 ± 0.0617	-0.08 ± 0.06	$(2.1 \pm 0.9)e + 31$	
HD 3266	656	8.8	16	0.0249 ± 0.0111	-0.40 ± 0.39	$(2.5 \pm 1.8)e + 28$	
G 103-50	615	23.1	127	0.0438 ± 0.0128			non-ID
G 88-10	713	0.3	16	< 0.0126		$< 4.0e + 29$	
G 89-14	688	1.1	46	< 0.0152		$< 1.4e + 29$	
HD 64606	595	1.6	47	< 0.0092		$< 1.6e + 28$	
HD 85091	635	215.4	13	0.2789 ± 0.0287	0.11 ± 0.10	$(1.6 \pm 0.7)e + 30$	
BD +30 2130	421	15.0	30	0.0772 ± 0.0211	-0.33 ± 0.25	$(1.5 \pm 0.8)e + 30$	
BD +21 2321	701	1.8	45	< 0.0167		$< 3.0e + 29$	
HD 108754	568	2.9	117	< 0.0332		$< 1.5e + 28$	
G 206-34	1124	1.0	176	< 0.0076		$< 1.9e + 29$	
BD +10 3711	776	0.1	72	< 0.0065		$< 6.6e + 28$	
BD +17 4708	627	2.3	145	< 0.0224		$< 9.5e + 29$	
HD 89499	391	96.8	76	0.1807 ± 0.0297	0.79 ± 0.10	$(1.3 \pm 0.6)e + 31$	
HD 224621	518	0.3	361	< 0.0158			
HD 6308	621	0.0	103	< 0.0211			
HD 6286	748	239.6	11	0.2383 ± 0.0244	0.82 ± 0.07	$(1.1 \pm 0.5)e + 30$	
HD 24202	734	0.7	130	< 0.0093			
HD 29907	1142	1.2	214	< 0.0092		$< 9.8e + 29$	
HD 30229	1156	1.2	58	< 0.0067			
HD 274680	1198	1.6	120	< 0.0131			
BD +5 3080	776	4.5	14	< 0.0333		$< 2.3e + 28$	
HD 175706	379	0.5	204	< 0.0172			
CD -37 14010	516	0.0	113	< 0.0199			
BD -00 4234	483	270.0	12	0.4094 ± 0.0390	-0.28 ± 0.09	$(3.0 \pm 1.3)e + 29$	
HD 245	1054	2.2	450	< 0.0079		$< 6.3e + 28$	
HD 20507	920	15.4	80	0.0404 ± 0.0115			ID?
HD 23439B	705	2.0	346	< 0.0210		$< 1.3e + 28$	
G 87-47	738	1.2	19	< 0.0097		$< 3.2e + 28$	
G 236-38	1055	0.1	68	< 0.0039		$< 9.0e + 28$	
G 176-27	718	1.2	15	< 0.0117		$< 4.5e + 28$	
BD +36 2193	421	2.5	27	< 0.0240		$< 1.3e + 29$	
G 178-56	1221	0.1	99	< 0.0040		$< 6.2e + 28$	
G 262-14	1600	0.7	220	< 0.0064		$< 5.3e + 28$	
HD 195987	1294	8.5	19	0.0115 ± 0.0048	-1.00 ± 0.83	$(1.7_{-1.7}^{+2.6})e + 27$	soft
G 230-45	1689	0.0	110	< 0.0049		$< 3.7e + 28$	
HD 200077	1022	0.0	73	< 0.0085		$< 2.9e + 28$	
G 215-47	1144	0.0	192	< 0.0097		$< 4.5e + 29$	
G 190-10	818	0.0	72	< 0.0087		$< 7.0e + 28$	
G 217-2	867	0.0	103	< 0.0120		$< 5.6e + 29$	
G 171-23	638	0.0	165	< 0.0086		$< 7.7e + 29$	
BD +13 308	698	30.1	319	0.0523 ± 0.0133			non-ID
BD +15 150	696	1.9	24	< 0.0123			
BD +47 451	352	0.0	94	< 0.0117		$< 9.8e + 28$	
BD +48 476	478	1.2	64	< 0.0101			
BD +27 335A	494	1.0	157	< 0.0190			
BD +27 335B	494	1.0	138	< 0.0189			
BD +43 538	928	1.0	159	< 0.0091			
HD 17841	860	4.3	34	< 0.0274			
HD 20039	928	0.4	212	< 0.0063		$< 1.2e + 29$	

Table 2. (continued)

Name	Exposure (s)	ML	Δ (")	counts (s ⁻¹)	HR	L_X (erg s ⁻¹)	Notes
HD 22694	604	80.5	0	0.1442 ± 0.0219	0.02 ± 0.15	$(5.8 \pm 2.6)e + 28$	
HD 30455	732	1.8	162	< 0.0143		$< 9.5e + 28$	
BD +72 245	759	6.6	76	< 0.0306		$< 1.0e + 29$	
BD +4 865	696	1.3	23	< 0.0103		$< 2.1e + 29$	
G 86-40	743	0.6	277	< 0.0109		$< 2.2e + 29$	
G 99-52	764	0.3	75	< 0.0062		$< 1.7e + 29$	
BD +38 1670	648	10.6	10	0.0256 ± 0.0107	0.21 ± 0.39	$(8.8 \pm 5.4)e + 28$	
BD +46 1314	740	3.0	41	< 0.0159			
BD +20 2030	699	1.1	209	< 0.0170		$< 4.5e + 29$	
BD +52 1397	624	0.4	45	< 0.0084			
BD +0 2627	621	1.0	34	< 0.0123		$< 1.0e + 29$	
G 253-41	808	0.5	815	< 0.0096		$< 3.1e + 29$	
G 253-44	819	1.3	308	< 0.0148		$< 2.0e + 29$	
G 176-46	447	0.3	142	< 0.0103		$< 1.6e + 29$	
HD 106516	679	35.9	13	0.0594 ± 0.0134	-0.54 ± 0.18	$(1.4 \pm 0.7)e + 28$	
BD +28 2137	786	1.1	64	< 0.0117		$< 2.8e + 30$	
BD +21 2442	748	7.9	27	0.0245 ± 0.0098	-0.05 ± 0.37	$(2.1 \pm 1.3)e + 28$	
G 62-40	525	4.1	181	< 0.0322		$< 1.3e + 30$	
G 178-27	1049	1.3	150	< 0.0190			
G 66-59	596	4.3	92	< 0.0309		$< 1.1e + 30$	
HD 149162	814	129.2	18	0.1718 ± 0.0209	-0.12 ± 0.12	$(1.1 \pm 0.5)e + 29$	
HD 157948	1407	3.7	35	< 0.0137		$< 4.8e + 27$	
G 183-9	823	4.9	170	< 0.0234			
G 262-32	1584	2.2	112	< 0.0066		$< 2.4e + 28$	
HD 200580	746	1.1	166	< 0.0127		$< 1.4e + 30$	
BD +11 4725	434	0.3	83	< 0.0148		$< 4.2e + 28$	
G 18-54	286	0.1	140	< 0.0176			
HD 218568	576	1.7	125	< 0.0125		$< 3.4e + 28$	
BD +38 4955	999	0.3	78	< 0.0071		$< 2.5e + 27$	
G 29-71	697	1.7	38	< 0.0059		$< 1.1e + 30$	
BD +33 4813	592	0.6	250	< 0.0117			

Columns: (1) Stellar identification, (2) RASS exposure time, (3) Maximum Likelihood, (4) difference between optical and X-ray position, (5) PSPC countrate, (6) 1σ countrate error, (7) hardness ratio, (8) 1σ hardness ratio error, (9) X-ray luminosity.
Abbreviations: non-ID: X-ray source not identical with Pop II star; soft: detection only in the soft band;

Instead, the X-ray detection for BD +13 308 is close to the position of MRK 1146. Similarly, the two X-ray detections in the hard bandpass only, CD -37 14010 and HD 23439B, are $6'$ and $8'$, respectively, from their optical positions, so we discount them as identifications. Finally, HD 20507 is a marginal case: Its proper motion is not sufficiently high to explain the large positional offset ($80''$), but the X-ray source properties (i.e., the X-ray luminosity and the hardness ratio) are consistent with what would be expected for a long-period binary. We choose to be conservative and not add this star to the sample of true identifications. In summary, we detect 13 out of 86 Pop II binaries in the RASS, which corresponds to a detection rate of 15%. HD 195987 is detected only in the soft band and its X-ray properties as given in Table 2 refer to this bandpass only.

Consequently, 73 systems in our Pop II sample are not detected in X-rays at the chosen detection threshold. Because the detection algorithm allows the X-ray position to vary, it will find an X-ray peak in any case, and the ML value will always be > 0

(note, that a value of $ML = 0.0$, as quoted in Table 2, is accurate only to the first digit). However, for most of the non-detections the X-ray peak is actually too far away from the optical position to be associated with the Pop II star.

The countrates are obtained by dividing the number of counts as determined by the ML algorithm by the exposure time corrected downward for telescope vignetting. Since the off-axis vignetting depends strongly on photon energy, different correction factors are applied to the exposure time of the soft, hard, and total bandpasses. The hardness ratios are defined as $HR = (H - S)/(H + S)$, with H and S being the countrates in the hard and soft bandpasses. For all stars in our sample, the number of counts obtained in the RASS is not sufficient to determine the spectral shape of the X-ray flux. Therefore, X-ray flux is obtained by multiplying the countrate by a conversion factor which assumes a spectral distribution. Clearly, a conversion factor which depends on hardness ratio would be best. For coronal sources observed with the ROSAT/PSPC,

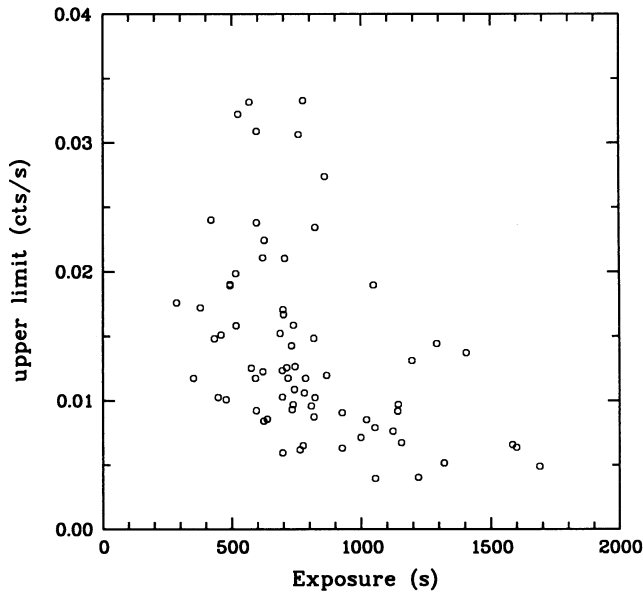


Fig. 1. Upper limits to the PSPC countrate (99.91% confidence) as a function of exposure time for undetected Pop II binaries.

the HR-dependent conversion factor was determined by Fleming et al. (1995) as $CF = (8.31 + 5.30HR) \cdot 10^{-12} \text{ erg cm}^{-2} \text{ ct}^{-1}$, where interstellar absorption is neglected. This conversion factor, along with the distances given in Table 1, are used to derive the luminosities given in Table 2. For non-detections, we use the same conversion factor evaluated at the mean hardness ratio of the detections, $\overline{HR} = -0.05$. Due to differences in the exposure time and the X-ray background over the sky, the limiting detectable X-ray flux varies strongly at the positions of the individual Pop II stars. As shown in Fig. 1, the limiting PSPC countrate ranges from 0.004 ct s^{-1} for exposures $> 1000 \text{ s}$ up to 0.03 ct s^{-1} for exposures $< 700 \text{ s}$. This corresponds to a limiting energy flux of about $0.3 - 2.4 \cdot 10^{-13} \text{ erg cm}^{-2} \text{ s}^{-1}$. Depending on stellar distance, we obtain limiting X-ray luminosities between $L_X \sim 2 \cdot 10^{27} - 3 \cdot 10^{30} \text{ erg s}^{-1}$.

5. X-ray luminosity function

5.1. The entire Pop II sample

For those Pop II binaries in our sample which have X-ray luminosities, we computed the cumulative X-ray luminosity distribution function (XLDF). The XLDF was derived using the Kaplan-Meier Product Limit Estimator which includes the information contained in the upper limits (e.g., Schmitt 1985). The resulting XLDF is shown in Fig. 2. First, the median of the distribution $\mu = 27.23$, which is coincident with the least luminous X-ray detection. However, as there are only few detections at low X-ray luminosities, the median is not very robust. To be precise, we can only say that the median lies below $\log L_x = 28.1$. If, for comparison, the XLDF were calculated by taking into account only the detections, but not the upper limits, then the median would lie at $\mu = 29.02$. This indicates that the XLDF of the whole Pop II sample is dominated by

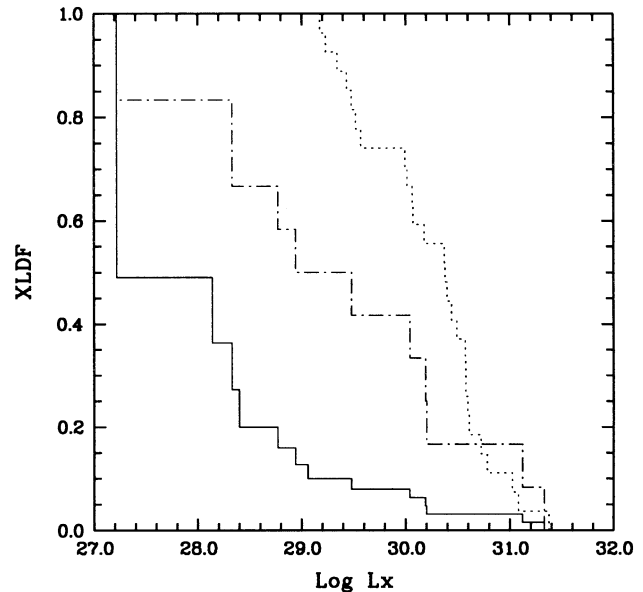


Fig. 2. Cumulative X-ray luminosity distribution function for the entire sample of Pop II binaries (solid curve), for the emission Pop II subsample (dashed-dotted curve), and for a complete sample of RS CVn binaries (dotted curve). The XLDF at the position $\log L_x$ gives the probability that a star has an X-ray luminosity $\geq \log L_x$.

upper limits rather than by X-ray detections. Second, despite the low detection rate, the median of the distribution still lies within the luminosity interval spanned by the X-ray detections. This is due to the fact that the upper limits are distributed over a large luminosity range as a result of the different exposure times and background levels, instead of being concentrated at low X-ray luminosities, as would be the case for a more homogeneous sample of observations (e.g., stellar clusters). Third, since the median denotes the 50th percentile of the distribution function, half of the Pop II binaries have X-ray luminosities below the median. With $\mu \leq 28.1$, it follows that at least 50% of the Pop II stars have X-ray luminosities below $10^{28} \text{ erg s}^{-1}$. Fourth, Fig. 2 clearly shows that the XLDF has a high-luminosity tail, which extends over two orders of magnitude in luminosity between $\log L_x \sim 29 - 31 \text{ erg s}^{-1}$ and contains about 10% of the stars. This high-luminosity tail is essentially due to the fact that our sample of Pop II binaries is not complete (i.e., volume-limited), but contains too large a fraction of distant stars contributing high luminosities and upper limits. Therefore, we explicitly mention that the XLDF of Fig. 2 represents the luminosity function of all Pop II binaries known so far, hence being slightly biased towards higher luminosities, rather than the intrinsic one. We see no way to define a complete, volume-limited subsample out of the entire sample of Table 1. Thus, the intrinsic XLDF can be constructed only after significantly enlarging the present sample of Pop II binaries.

5.2. Comparing emission Pop II with RS CVn systems

The RS CVn systems constitute the most active class of late-type binaries (e.g., Schmitt et al. 1990, Dempsey et al. 1993).

Hall (1976) proposed the following definition: The classical RS CVn binaries have orbital periods between 1 – 14 d, show significant Ca II H & K line emission, and have a primary of spectral type F-G, V-IV. The long-period RS CVn systems have periods beyond 14 d, and a primary of type G-K IV-II. Hall (1976) notes that lightcurve variations are a characteristic but not required property of RS CVn systems (cf. Table 4 in Hall 1976). Consequently, the ‘emission Pop II’ systems, i.e. those stars in our spectral types F-K comprising sample which exhibit significant Ca II H & K line emission, may be considered the halo component analogs to the RS CVn systems of the Galactic disk. In a quantitative way, we define the emission Pop II as systems with a chromospheric index $A_k \geq 0.15$. Unfortunately, we know both chromospheric indices and X-ray luminosities for only a quarter of the Pop II sample stars. Therefore, our emission Pop II subsample is statistically not very significant, comprising only 12 systems – CD-48 1741, BD+13 13, HD85091, BD+30 2130, HD89499, HD6286, BD+5 3080, BD-00 4234, HD195987, HD22694, BD+38 1670, BD+21 2442 – amongst them being 10 X-ray detections. We note that for 8 out of the 12 emission Pop II systems observations to search for photometric variability have been performed. Lightcurve variations attributed to star spots have been reported for BD+13 13 (Rodono et al. 1994, Henry et al. 1995), for HD85091, BD+30 2130, BD-00 4234, HD22694 (Henry et al. 1995), and for HD6286 (Hooten and Hall 1990). Further, variability in the V-amplitude has been detected for HD89499 (Ardeberg and Lindgren 1991), which might be caused by star spots. Only for CD-48 1741, no significant light variability has been found (Lindgren et al. 1987). These results indicate at least half of our emission Pop II sample to have star spots; thus, also from the aspect of lightcurve variability a comparison with the RS CVn binaries seems to be justified.

The emission Pop II binaries and the RS CVn systems, as a class, significantly differ in proper motion, age, and (photospheric) metallicity. We note that the entire Pop II sample covers a metallicity range $-2.9 \leq [m/H] \leq -0.4$, and the emission Pop II sample covers $-2.1 \leq [m/H] \leq -0.4$. Randich et al. (1993,1994) also find many RS CVn binaries to be metal deficient with $-1.0 \leq [m/H] \leq 0$, but they note, as different [Fe/H] values are derived for the two components of several SB2 binaries, that “the spectral lines could be significantly affected by surface activity (spots and plages) and may not represent a true metal deficiency”. On the other hand, Fekel and Balachandran (1993) derive abundances $-0.25 \leq [m/H] \leq 0.10$ for a sample of 10 SB1 RS CVn binaries. Specifically, for 4 stars common in both samples, abundances much closer to the solar photospheric values were derived by Fekel and Balachandran (1993). Assuming the RS CVn to belong to the disk population, then, from a theoretical point of view, one would expect photospheric abundances close to solar due to their spatial proximity. Thus, although there may be a small overlap in metallicity between the Pop II and the RS CVn binaries, which is difficult to quantify at present, the metallicity ranges covered by the two stellar classes are distinctly different.

The XLDF of the emission Pop II subsample is shown in Fig. 2. The median $\mu \sim 29.2$, but is not very well constrained due to the small sample size. Next, we constructed the XLDF for a complete, volume-limited sample of RS CVn binaries. The sample of all RS CVn systems known so far, which has been compiled by Strassmeier et al. (1988) and analyzed in X-rays using the RASS by Demspey et al. (1993), is estimated to be complete out to a distance of about 50 pc (Drake et al. 1989, Ottmann and Schmitt 1992). Selecting those stars within 50 pc, we find 27 systems, all of which are detected in the RASS. In Fig. 2, we plot the XLDF of the complete RS CVn subsample. Obviously, the median of the emission Pop II XLDF is about one order of magnitude smaller than that of the RS CVn sample, while its width is much broader. For a complete sample of Pop II binaries, the median is expected to be even lower, and the width substantially smaller. Thus, the emission Pop II halo binaries typically are at least one order of magnitude, probably more, less X-ray luminous than the disk component RS CVn binaries. But the high-luminosity tail of the emission Pop II XLDF is entirely within the luminosity range of the RS CVns, indicating that the most luminous emission halo binaries have X-ray luminosities as high as those of the most active disk binaries.

6. Which properties determine the X-ray activity?

For the Pop II binaries, the photometric properties $B - V$ and M_V of the secondary are unknown. Thus, we do not know whether the secondary contributes at all to the total X-ray luminosity or if it is even the more active component. For this reason, we use the integral luminosity L_x as the activity measure, not the more desirable surface flux F_X or the normalized luminosity L_x/L_{bol} . For the same reason, we correlate L_x with other integral quantities rather than parameters referring to the primary alone. Therefore, amongst the photospheric parameters, we correlate only the metallicity with L_x , assuming that both stellar components have the same [m/H]. Similarly, we use the orbital period P_{orb} (corresponding to the rotational period in case of synchronous rotation) as rotational parameter, because the projected rotational velocity $v \sin i$ is unknown for most systems, and the rotational velocity or the Rossby number can, at best, be estimated only for the primary.

6.1. X-ray activity vs. rotation

Under the assumption of synchronous rotation, P_{rot} can be used as the rotational parameter even when the active component is unknown. In short-period (SP) systems, the stellar components will rotate synchronously due to the strong tidal coupling and the resulting short synchronization timescale. The division between SP and long-period (LP) systems is made at $P_{orb} = 20$ d on the grounds that (i) subgiant systems with $P_{orb} \leq 20$ d are expected to be closely synchronized ($P_{rot} \simeq P_{orb}$) on evolutionary time scales (Zahn 1977), and (ii) Latham et al. (1992) have found for extreme metal-poor systems the longest-period circular orbit, which gives a lower limit of the longest-period synchronized orbit, to be at a period of about 19 d. In LP binaries, the rota-

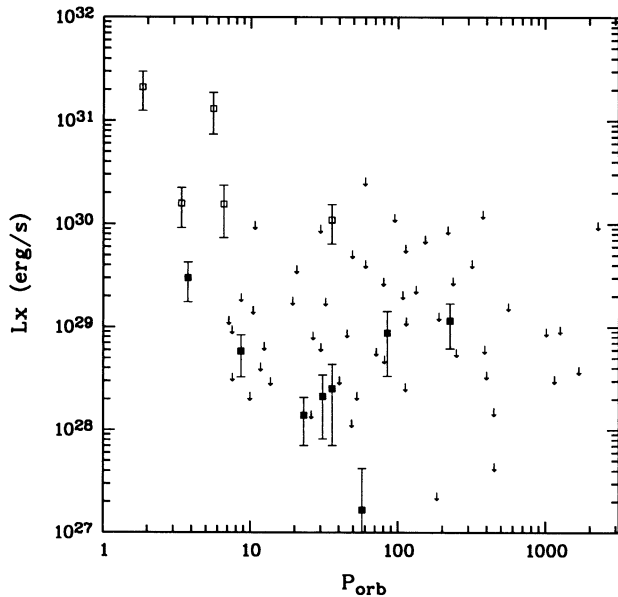


Fig. 3. X-ray luminosity plotted against orbital period for the X-ray detections (*squares*) and upper limits (*arrows*). Amongst the X-ray detections, we indicate those systems known to be evolved (*open squares*); the other detections are known or presumed to be dwarfs (*filled squares*). Note that all highly active detections are evolved, while all the less active detections are dwarfs.

tional period may still be close to the orbital one, except for very long-period systems having correspondingly long synchronization timescales and, therefore, $P_{rot} > P_{orb}$. However, all the detected Pop II systems, except HD149162, have orbital periods $P_{orb} \leq 85$ d and, thus, are synchronous rotators or, at least, do not deviate too strongly from synchronism. The X-ray activity of the very long-period binary HD149162 ($P_{orb} = 226.3$ d) comes very likely from the secondary, which is itself a binary system with a presumably much shorter period.

In Fig. 3, the X-ray luminosity is plotted as a function of orbital (or, for the SP systems, rotational) period. At first glance, it is surprising that we did not detect all the SP systems, but did detect 7 LP systems. Specifically, all the four SP systems with $P_{rot} \leq 6$ d, BD+13 13, HD85091, HD89499, and BD-00 4234, have been detected, while there are only 2 detections, BD+30 2130 and HD 22694, among the 16 systems with $6 < P_{rot} \leq 20$ d. The detected LP systems, HD3266, HD6286, HD195987, BD+381670, HD106516, BD+212442, and HD149162, have rotational periods up to 226 d. For some LP systems, the X-ray activity may be naturally explained: As mentioned above, the secondary of HD149162 is probably a SP binary. HD6286 is evolved; therefore, despite its longer period, it may have a high rotational velocity $v_{rot} = R/P_{rot}$ and hence a large X-ray luminosity. Finally, HD195987 could possess a white-dwarf (WD) companion, because its X-ray emission is typical for WDs with respect to both the magnitude ($L_x = 1.7 \cdot 10^{27}$ erg s $^{-1}$) and softness ($HR = -1.0$; Fleming et al. 1996). However, HD106516 and presumably also HD3266,

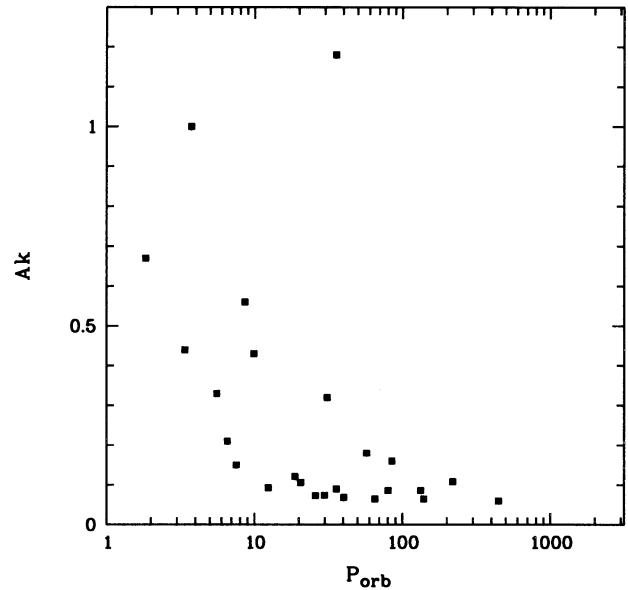


Fig. 4. Chromospheric index A_k as a function of orbital period.

BD+381670, and BD+212442 are dwarfs, thus having low rotational velocities.

For comparison, the chromospheric index A_k is plotted as a function of orbital period in Fig. 4. The correlation between A_k and P_{orb} has already been investigated by Pasquini and Lindgren (1994). In Fig. 4, we have added our new A_k measurements. On the basis of this extended data set, we confirm the result found by Pasquini and Lindgren (1994) that systems with P_{orb} less than about 10 d show chromospheric activity, while systems with longer periods typically possess no active chromospheres unless they are evolved (e.g., HD 6286). However, there seem to be a few exceptions to this trend, since we find evidence for chromospheric activity in BD+212442, HD195987, BD+381670, and HD149162. This result is consistent with our finding of coronal activity in these systems. The correlation between chromospheric and coronal activity will be studied below in detail.

Obviously, the X-ray luminosity is not very strongly correlated with the orbital period. The fact, that all the highly X-ray luminous systems are evolved (cf. Fig. 3), indicates that the X-ray luminosity depends not only on the orbital (or rotational) period, but also on the stellar surface, or radius. Therefore, it may be more appropriate to compare the rotational velocity, which involves both period and radius, rather than the period, to the X-ray luminosity of stars of different luminosity classes. In Fig. 5a, the X-ray luminosity is plotted as a function of the projected rotational velocity for all stars with known $v \sin i$ values. Unfortunately, $v \sin i$ values have been measured only for 18 sample stars (Spite et al. 1994, Henry et al. 1995), of which 7 are X-ray detections. Evidently, all the non-detections have rotational velocities $v \sin i$ below 8 km s $^{-1}$, while the detections typically have higher $v \sin i$ values with $5 \leq v \sin i \leq 23$. However, the data are too sparse to allow firm conclusions about the correlation between L_x and $v \sin i$.

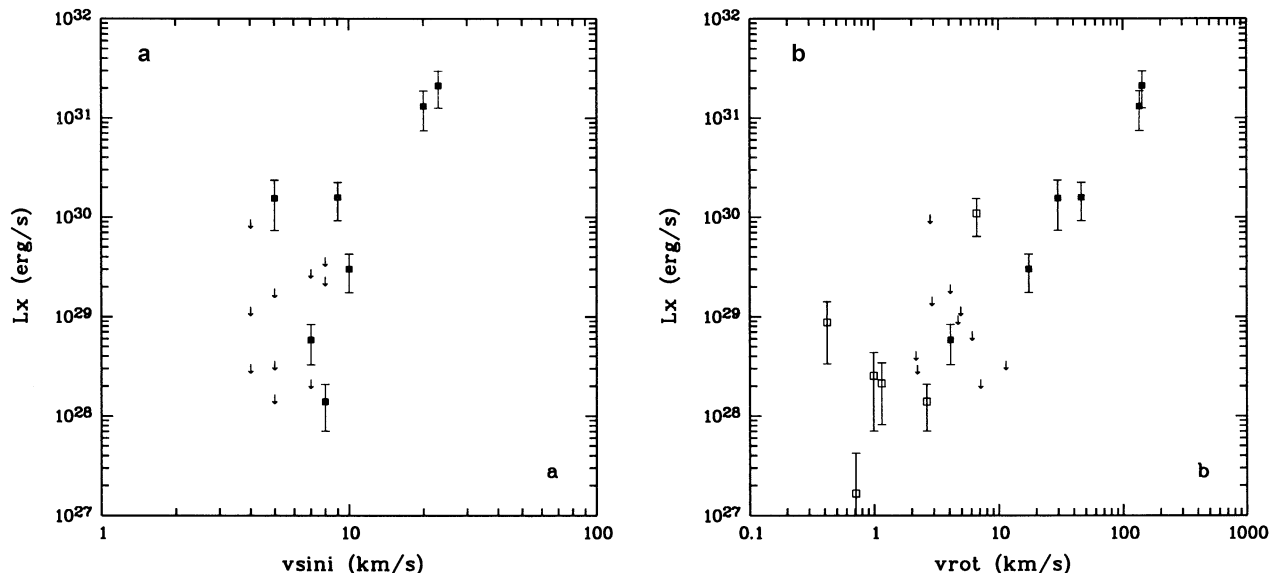


Fig. 5. **a** X-ray luminosity vs. projected rotational velocity for all sample stars with known $v \sin i$. **b** X-ray luminosity vs. rotational velocity of the primary for all X-ray detections (*open squares* indicate LP systems, *filled squares* SP systems) and the SP non-detections (*arrows*). HD 149162 is not included in this figure, because its secondary is itself a probably SP binary.

In Fig. 5b, the X-ray luminosity is shown as a function of the rotational velocity v_{rot} of the primary for the X-ray detections and the SP non-detections. The rotational velocities, listed in Table 3, are derived from the relation $v_{rot} = 2\pi R_{primary}/P_{orb}$, with the radius of the primary being determined from the evolutionary models of Van den Berg and Bell (1985). The $v \sin i$ values are, for the most part, lower than the corresponding v_{rot} values, as would be expected due to the projection effect. The rotational velocity is a better intrinsic rotational parameter than $v \sin i$, because it does not suffer from the projection effect and, consequently, it covers a more extended parameter range compared to the rather narrow range of $v \sin i$ values. However, one has to keep in mind that the primary might not be in any case the active component and its radius is not known very accurately. These uncertainties lead to an additional scatter in the activity-rotation relation. Nevertheless, for the X-ray detections, the X-ray luminosity obviously correlates better with the rotational velocity than with the orbital period. This is shown quantitatively by calculating the correlation probability of these quantities for the X-ray detections (except HD149162): The linear correlation probability (cf. Bevington 1969) between $\log L_x$ and $\log v_{rot}$ ($\log P_{orb}$) amounts to 0.9999 (0.9935). It is interesting to note that the RS CVn systems seem to show a similar correlation between rotation and activity as the Pop2 binaries. Drake et al. (1989) found that, for the RS CVn systems, the 6 cm radio luminosity, which is correlated significantly with the X-ray luminosity and is thus a good measure of activity, does not show any significant correlation with either orbital or rotational period; instead, a fair correlation with the rotational velocity of the active component was found.

The SP binaries and the evolved LP system HD 6286 have moderately high rotational velocities $v_{rot} > 4 \text{ km s}^{-1}$. The detected LP dwarf systems have low rotational velocities

around $v_{rot} \sim 1 \text{ km s}^{-1}$, which however might be sufficient to maintain activity levels of $L_x \sim 10^{28} \text{ erg s}^{-1}$. Fig. 5b further shows that the SP non-detections have rotational velocities $v_{rot} \sim 1 - 10 \text{ km s}^{-1}$, from which we would expect X-ray luminosities $L_x \sim 10^{27} - 10^{29} \text{ erg s}^{-1}$ according to the rotation-activity relation for optically selected (i.e., mostly non-saturated) stars (Pallavicini et al. 1981). Clearly, some of the non-detected SP systems have upper limits greater than this, indicating a short exposure and/or high background as the explanation for why they were not detected. But a few non-detected SP systems have upper limits which indicate X-ray luminosities $L_x < 10^{28} \text{ erg s}^{-1}$, which would be inconsistent with the L_x - v_{rot} relation. Longer pointed observations are required to decide whether these systems actually deviate from the rotation-activity relation, or whether the associated parameters are too uncertain.

6.2. X-ray activity vs. metallicity

In Fig. 6, we plot the X-ray luminosity versus the metallicity. Twelve out of the 13 X-ray detections have intermediate metallicities with $[m/H] \geq -1.4$, while there is only one X-ray detection (HD 89499) amongst the extreme Pop II stars. Thus, the detection rate is much lower for the extreme metal-poor stars than for the intermediate Pop II. Just to illustrate, if the line between the two metallicity groups would be drawn at $[m/H] = -1.4$, then the detection rate would be 24% and 3% for the intermediate and the extreme Pop II systems, respectively. One may ask whether the different detection rates are actually caused by observational and/or intrinsic biases: First, systematically shorter RASS exposures times for the extreme Pop II subsample, as would arise from a concentration towards the ecliptic plane, are not present; both metallicity groups have

Table 3. Derived rotational velocities v_{rot} for all the SP and LP X-ray detections (except HD 149162) and the SP non-detections with known distances. If available, the measured v_{sini} values (Spite et al. 1994, Henry et al. 1995) are given for comparison.

Name	P_{orb} (d)	$R_{primary}$ (R_{\odot})	v_{rot} (km s^{-1})	v_{sini} (km s^{-1})
BD+13 13	1.84	5.20	143.8	23
HD3266	36.00	0.70	0.99	-
HD85091	3.39	3.10	46.54	9
BD+30 2130	6.57	3.90	30.21	5
HD89499	5.57	15.00	137.0	20
HD6286	35.70	4.70	6.70	-
BD-00 4234	3.76	1.30	17.60	10
HD195987	57.32	0.80	0.71	-
HD 22694	8.65	0.70	4.12	7
BD+38 1670	85.05	0.70	0.42	-
HD 106516	23.10	1.20	2.64	8
BD+21 2442	31.02	0.70	1.15	-
HD111980	12.43	1.50	6.14	7
CD-48 1741	7.56	1.70	11.44	5
BD+5 3080	9.94	1.40	7.17	7
G87-47	13.73	0.60	2.22	-
G176-27	11.73	0.50	2.17	-
BD+36 2193	7.15	0.70	4.98	4
BD+72 245	7.53	0.70	4.73	-
BD+4 865	8.66	0.70	4.11	-
G176-46	10.44	0.60	2.92	-
G66-59	10.74	0.60	2.84	-

about the same mean exposure time. Second, the extreme Pop II systems are located on average at larger distances than the intermediate Pop II. Consequently, the extreme metal-poor sample has on average higher luminosity upper limits than the intermediate Pop II, as is evident from Fig. 6. Third, the extreme metal-poor stars might have systematically longer rotation periods, and hence lower levels of X-ray activity. To check this suspicion, we show the correlation between metallicity and orbital period in Fig. 7. Obviously, the intermediate Pop II systems cover a more extended range of periods than the extreme Pop II. But, the fraction of SP systems is only moderately larger for the intermediate Pop II than for the extreme Pop II stars shown in Fig. 6 and 7 (28% compared to 22%). Thus, there is no obvious metallicity-period correlation which would explain the higher detection rate of the intermediate Pop II stars.

Since our upper limits are rather conservative, we conclude from Fig. 6 that the majority of the extreme Pop II stars have X-ray luminosities below 10^{29} erg s^{-1} , although HD 89499 has an extremely high L_x . In contrast, the X-ray luminosities of the intermediate systems apparently are distributed more homogeneously over 4 orders of magnitude. Therefore, intermediate and extreme Pop II stars may have different X-ray luminosity functions. As there is only one X-ray detection amongst the extreme Pop II systems, their XLDF cannot be computed at the present stage. Thus, firm conclusions can be drawn only after further detections of extreme metal-poor systems.

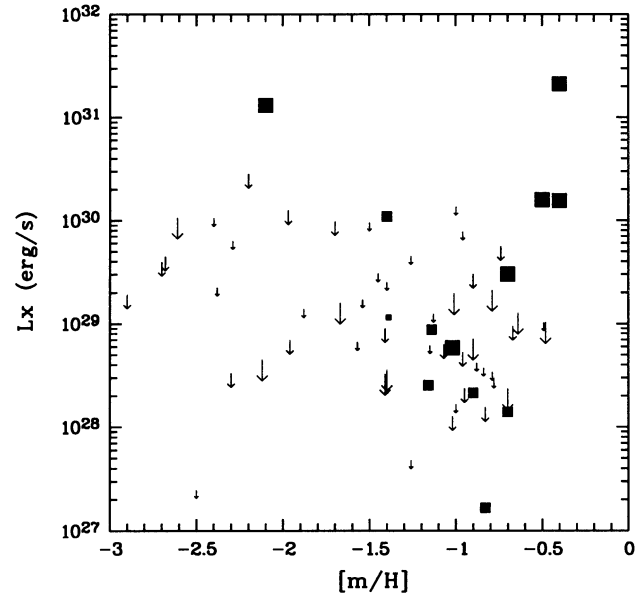


Fig. 6. X-ray luminosity plotted against metallicity for the X-ray detections (filled squares) and upper limits (arrows). Orbital periods between 1 – 20 (20 – 100, > 100) d are marked by large (intermediate, small) symbols. HD 149162 with $P_{orb} = 226.3$ d has probably a SP secondary.

Fig. 8 shows the hardness ratio as a function of metallicity. Very low hardness ratios of $HR \sim -1$ indicate coronae having only a cool temperature component with $T \sim 10^6$ K or a WD. Intermediate values of the hardness ratio are representative of coronae which have a hot temperature component with $T \sim 10^7$ K, i.e. the hardness ratio increases with temperature and with the emission measure ratio between the high and low temperature components. Very high hardness ratios of $HR \sim +1$ will be obtained only for X-ray spectra with very high temperatures and high absorption. Fig. 8 shows that the intermediate Pop II stars typically have slightly negative hardness ratios centered around $HR \sim -0.1$, indicating coronal temperatures around 10^7 K and low interstellar absorption. In contrast, the extreme metal-poor system HD 89499 has a distinctly higher hardness ratio of $HR = 0.79$, indicating correspondingly high coronal temperatures and high interstellar absorption. Indeed, ASCA SIS and ROSAT PSPC spectra have shown HD 89499 to have a coronal temperature of 27 million K and $N_H = 3.6 \cdot 10^{20} \text{ cm}^{-2}$ (Fleming and Tagliaferri 1996). The high coronal temperature of HD 89499 is consistent with our theoretical understanding that extreme metal-poor coronae can not release their energy by line emission, but only by thermal bremsstrahlung, which is efficient above 20 million K. HD 6286, being on the boundary between intermediate and extreme Pop II, is the only other star with a similarly high hardness ratio, $HR = 0.82$, again indicating a high temperature and N_H value (therefore, its distance is probably somewhat larger than $d = 55$ pc as quoted in Table 1). Again, it requires the detection of more extreme metal-poor stars to draw conclusions about a correlation between metallicity and coronal temperature.

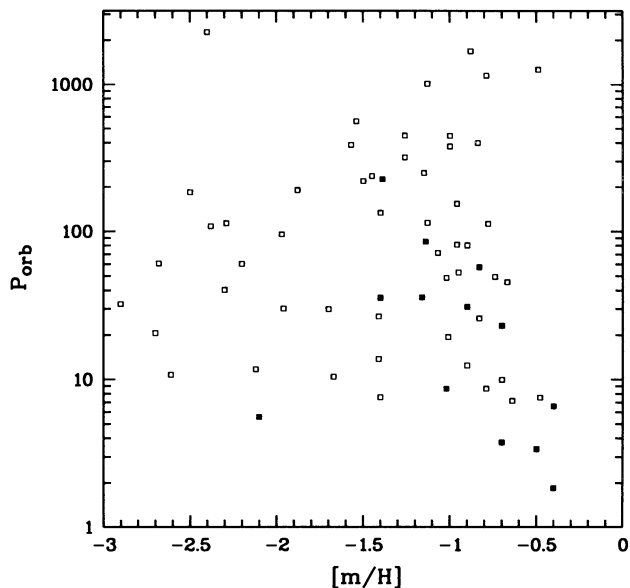


Fig. 7. Correlation between metallicity and orbital period for those Pop II stars with known distances (i.e., the same stars as in Fig. 6). The X-ray detections are marked by *filled squares*, the upper limits by *open squares*. Again, HD 149162 with $P_{orb} = 226.3$ d has probably a SP secondary.

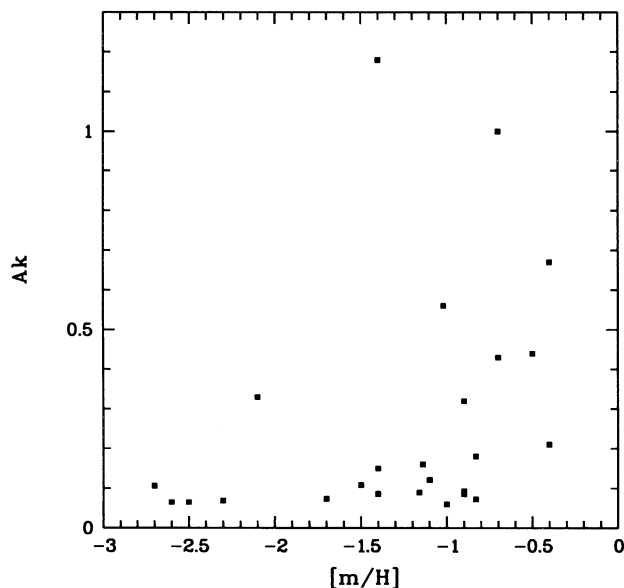


Fig. 9. Chromospheric index shown as a function of metallicity.

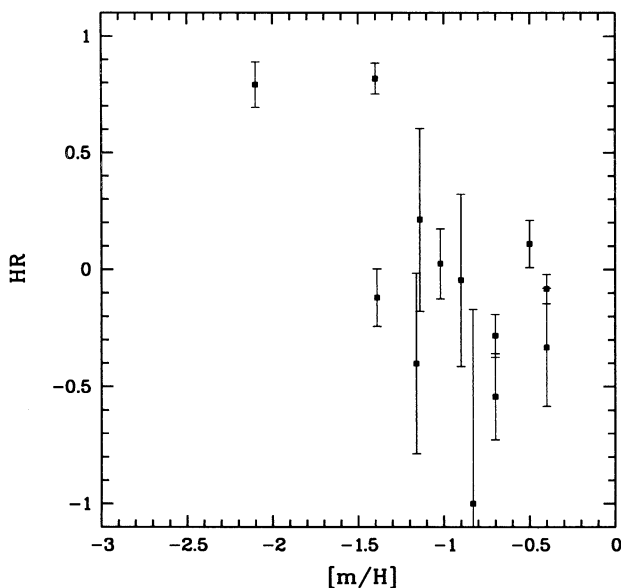


Fig. 8. Dependence of the hardness ratio on the metallicity.

In Fig. 9, the dependence of the chromospheric indices A_k (cf. Sect. 2) on the metallicity is shown. Clearly, the Pop II binaries with metallicities larger than about $[m/H] \sim -1.4$ exhibit on average significantly higher chromospheric activity levels than the systems with lower metallicities. Hence, chromospheric activity shows the same dependence on metallicity as coronal activity. Thus, for the extreme Pop II binaries, the chromospheric and coronal activity apparently is reduced compared to the intermediate metallicity systems.

6.3. X-ray activity vs. atmospheric structure

In this section, we investigate the dependence of the X-ray activity on other atmospheric parameters. First, we correlate the X-ray luminosity with the hardness ratio as an indicator of the coronal temperature (cf. Sect. 6.2). Second, we study the relation between the coronal and chromospheric activity levels. However, a possible correlation between the coronal activity measure L_x and the chromospheric index A_k may be obscured by a large scatter for the following reasons: (i) L_x is an integral property while A_k is normalized to the stellar surface flux. (ii) A_k is only a relative activity index and not the absolute Ca II K line flux. (iii) The X-ray and optical data are not taken simultaneously but are spread over an interval of a few years, during which time the activity levels may have changed.

In Fig. 10, the X-ray luminosity is plotted as a function of the hardness ratio for the 13 detected Pop II systems. There appears to be only a weak correlation between L_x and HR. Actually, one would expect a correlation between L_x (or F_x) and T , as it was observed in several previous studies. For example, for a sample of 130 late-type stars detected by the EINSTEIN IPC, Schmitt et al. (1990) found the X-ray luminosity to be correlated with the temperature obtained in a single-temperature fit according to $L_x \propto T^{2.5}$. Furthermore, for a sample of late-type stars covering a large range of activity levels, Ottmann (1993) derived a relation between more physical quantities, the stellar surface flux and the maximum loop temperature, which was $F_x \propto T_{max}^{3.5}$. However, the hardness ratio is not linearly correlated with the coronal temperature, because it depends on both the emission measure and the temperature in the case of two-temperature fits, and it is also affected by interstellar absorption.

Fig. 11 shows the dependence of the X-ray luminosity on the chromospheric index for all the X-ray detections and upper limits for which both the A_k values and the distances are known.

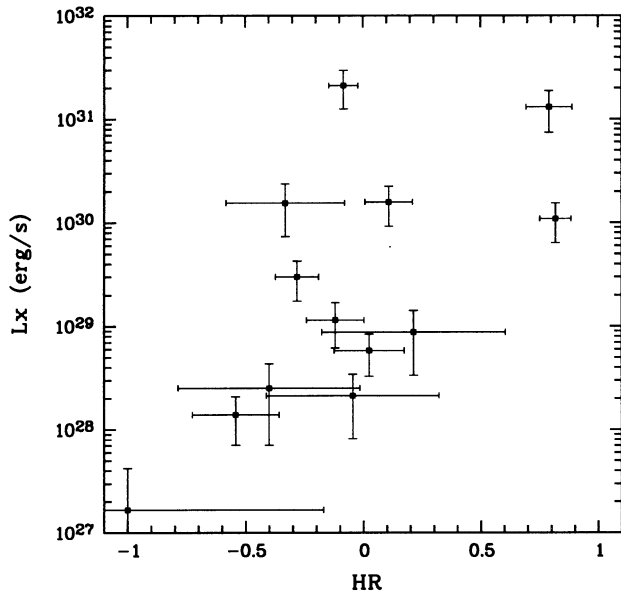


Fig. 10. X-ray luminosity vs. hardness ratio for the 14 X-ray detections.

For the X-ray detections, the X-ray luminosity and the chromospheric index are correlated according to $\log L_x \propto \log A_k$, although there is a large scatter due to the reasons outlined above. The systems which were not detected in X-rays and, thus, have low L_x values, also have low A_k values. There is only one exception, BD+53080, which has quite a large A_k value and an X-ray luminosity less than $2 \cdot 10^{28} \text{ erg s}^{-1}$. Again, this discrepancy may arise from the facts that the A_k value does not represent the absolute chromospheric flux, and that the optical and X-ray data are not taken simultaneously.

7. Summary and Discussion

We have investigated the coronal activity of a sample of 86 Pop II field binaries using data from the RASS. Only 13 Pop II systems were detected; another system is a possible detection. X-ray luminosities and hardness ratios were derived for the X-ray detections, and upper limits were placed on X-ray luminosity for the non-detections. The key results of this study can be summarised as follows:

- (i) The XLDF of the entire sample, taking into account both detections and upper limits, has a median luminosity $\log L_x \leq 28.1$, indicating that the Pop II binaries typically have rather low X-ray luminosities. For a subsample of emission Pop II systems, which may be considered as the old, metal-poor analogs to the RS CVn binaries, the median is at $\log L_x \sim 29.2 \text{ erg s}^{-1}$. For comparison, a complete sample of RS CVn binaries detected in the RASS has a median luminosity $\log L_x = 30.38 \text{ erg s}^{-1}$. Thus, a complete sample of emission Pop II binaries would be at least one order of magnitude less X-ray luminous than the RS CVn binaries.
- (ii) The high-luminosity tail of the XLDF at $\log L_x \sim 29 - 31 \text{ erg s}^{-1}$ demonstrates that Pop II binaries can maintain coronal activity levels as high as those of the RS CVn binaries.

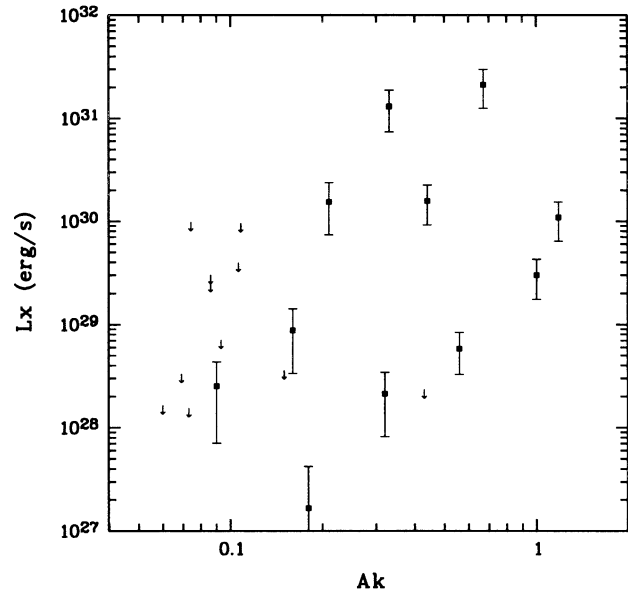


Fig. 11. X-ray luminosity vs. chromospheric index for all the X-ray detections and upper limits for which both A_k values and distances are known.

(iii) Twelve out of the 13 X-ray detections have intermediate metallicities with $[m/H] \geq -1.4$, while there is only one extreme metal-poor detection (HD 89499). This possibly indicates that extreme Pop II binaries have typically lower X-ray luminosities than intermediate Pop II. Further, HD 89499 has a higher hardness ratio, and hence higher coronal temperature, than the intermediate Pop II systems typically have. This high coronal temperature is consistent with the idea that extreme metal-poor coronae can release their energy only by thermal bremsstrahlung, which is efficient above 20 million K.

(iv) The X-ray luminosity is not very well correlated with the rotational period. Specifically, only 6 (out of the 20) SP systems and 8 LP systems were detected. Thus, Pop II binaries can be strong X-ray emitters despite having long periods, a fact well known from Pop I binaries, especially if they are evolved. On the other hand, Pop II binaries with short orbital periods are not necessarily strong X-ray emitters. In contrast, SP Pop I binaries are typically thought to be strong X-ray emitters.

As the emission Pop II systems cover the same range of spectral types, luminosity classes, and orbital periods as the RS CVn systems, but differ distinctly in metallicity and age, it is reasonable to associate their lower median X-ray luminosities with their lower values of metallicity, significantly higher ages, and probably lower fraction of evolved stars. The evolved Pop II systems in our sample have high X-ray luminosities of $\log L_x \sim 30 - 31 \text{ erg s}^{-1}$, while the dwarf Pop II systems have lower luminosities of $\log L_x \sim 27 - 29 \text{ erg s}^{-1}$. In contrast, the X-ray luminosities of the RS CVn binaries are, to first order, independent of the luminosity class; the dwarf RS CVn systems also possess X-ray luminosities of $\log L_x \sim 29 - 31 \text{ erg s}^{-1}$ (cf. Fig. 3 in Dempsey et al. 1993). Thus, the lower median X-ray

luminosity of the emission Pop II binaries may be explained in part by their lower fraction of evolved systems.

A comparison between RS CVn and emission Pop II binaries on the one hand, and between intermediate and extreme Pop II binaries on the other hand, indicates that the median X-ray luminosity possibly decreases with photospheric metallicity and/or age (a low photospheric metallicity also indicates a high age). Nevertheless, the extreme metal-poor, old system HD89499 is as X-ray luminous as the RS CVn systems. This suggests that, if at all, there is no linear relation between activity and metallicity/age. The relation between activity and photospheric metallicity might reflect primarily the radiation efficiency, which depends on coronal metallicity and temperature. The metallicities in stellar coronae may not be the same as in the photospheres. For example, in the Sun, the low first ionization potential (FIP) elements (Fe, Ca, Mg,...) are probably enhanced by a factor 4 in the corona compared to the solar photospheric values (FIP-effect; Meyer 1985). In contrast, the FIP-effect seems to be absent in Procyon (Drake et al. 1995). In the RS CVn binaries, the photospheric Fe abundances are possibly slightly sub-solar (cf. Sect. 5). Recent EUVE and ASCA observations have shown that the coronal Fe abundances of RS CVn and Algol-type binaries apparently are below the solar photospheric values by factors 2-4 typically (e.g., Schrijver et al. 1995, Singh et al. 1995, Stern et al. 1995, Singh et al. 1996), although these abundance determinations might be affected by the non-negligible optical thickness of the lines (e.g., Schrijver et al. 1994). Finally, in the Pop II binary HD 89499, the ASCA spectrum clearly shows the absence of emission lines (Fleming and Tagliaferri 1996). These abundance determinations indicate that the photospheric and coronal abundances typically do not differ by too large a factor, and that the photospheric metallicity may be used as a rough measure for the coronal metallicity. Therefore, for the RS CVn systems with slightly sub-solar photospheric metallicities, line emission is rather efficient in releasing the coronal thermal energy. Assuming that the intermediate Pop II systems with $-1.4 < [m/H] < -0.4$ have correspondingly lower coronal metallicities than the RS CVn, then the line emission is reduced in its efficiency. This might explain the lower activity levels of the intermediate Pop II systems. Extreme metal-poor systems are expected to radiate away their energy only via thermal bremsstrahlung, which requires extremely high temperatures to be efficient. Therefore, the extreme Pop II systems may have either high activity levels if their coronal heating rates are extremely high, or low activity levels even if their heating rates are moderately high.

For single stars, the effect of stellar age is primarily to decrease angular momentum due to magnetic braking, resulting in a decline in X-ray activity. Binary systems can maintain high rotation rates despite old age due to their synchronous rotation. Therefore, SP binaries are expected to have high activity levels, no matter how old they are. The Pop I SP binaries indeed are known to be strong X-ray emitters (e.g., RS CVns, Algols). An exception to this trend may be provided by the SP binaries of the old open cluster M67, for which a rather low detection rate (i.e., 1/11), indicating low coronal activity, was found by ROSAT

observations (Pasquini and Belloni 1994). In contrast, the Pop II SP binaries are not *per se* strong X-ray emitters. Surprisingly, even some of the emission Pop II SP systems have rather low X-ray luminosities: For the detected SP system HD 22694, an X-ray luminosity $L_x = 5.8 \cdot 10^{28} \text{ erg s}^{-1}$ was derived. For the non-detected SP systems CD-48 1741 and BD+53 080, upper limits of $< 3.6 \cdot 10^{28} \text{ erg s}^{-1}$ and $< 2.3 \cdot 10^{28} \text{ erg s}^{-1}$ were determined, indicating X-ray luminosities below 10^{28} erg/s despite their quite high rotational velocities of $v \sin i = 5$ and 7 (cf. Table 3). These luminosities are lower than expected from the rotation-activity relation for single stars (Pallavicini et al. 1981). The low coronal activity of CD-48 1741, BD+53 080, and possibly of further non-detected Pop II binaries might be associated with their long stellar ages, over which time the magnetic field may not have survived.

Acknowledgements. We thank Dr. J. Schmitt for helpful suggestions. We also thank the referee, Dr. T. Simon, for his careful reading of the manuscript and the many valuable suggestions, which definitely helped to improve the paper. This research has made use of the Simbad database, operated at CDS, Strasbourg, France. The Rosat project is supported by the Bundesministerium für Bildung, Wissenschaft, Forschung und Technologie (BMBF/DARA) and the Max-Planck-Society. This project is supported by the Deutsche Agentur für Raumfahrtangelegenheiten (DARA) GmbH under contract 50 OR 9612 0. TAF acknowledges support from NASA under grant number NAGW-3160.

References

- Abt + Willmarth 1987, ApJ, 318, 786.
- Ardeberg, A., Lindgren, H. 1991, A&A, 244, 310.
- Bevington, P.R. 1969, Data Reduction and Error Analysis for the Physical Sciences, McGraw-Hill, New York.
- Boesgaard, A.M., Steigman, G. 1985, ARA&A, 23, 319.
- Carney, B.W., Latham, D.W. 1987, AJ, 93, 116.
- Cruddace, R.G., Hasinger, G., Trümper, J., Schmitt, J.H.M.M., Hartner, G.D., Rosso, C., Snowden, S.L. 1989, Exp. Astron., 1, 365.
- Dempsey, R.C., Linsky, J.L., Fleming, T.A., Schmitt, J.H.M.M. 1993, ApJS, 86, 599.
- Drake, S.A., Simon, T., Linsky, J.L. 1989, ApJS 71, 905.
- Drake, J.J., Laming, J.M., Widing, K.G. 1995, ApJ 443, 393.
- Fekel, F.C., Balachandran, S. 1993, ApJ 403,708.
- Fleming, T.A., Molendi, S., Maccacaro, T., Wolter, A. 1995, ApJS, 99, 701.
- Fleming, T.A., Snowden, S.L., Pfeffermann, E., Briel, U., Greiner, J. 1996, A&A, in press.
- Fleming, T.A., Tagliaferri, G. 1996, ApJ, submitted.
- Gehren, T. 1982, The Messenger, 27, 22.
- Grenon, M. 1996, in Ninth Cambridge Workshop on Cool Stars, Stellar Systems, and the Sun, R. Pallavicini and A. Dupree (Eds.)
- Henry, G.W., Fekel, F.C., Hall, D.S. 1995, AJ 110, 2926.
- Hall, D.S. 1976, in IAU Colloq. 29, Multiply Periodic Phenomena in Variable Stars, W.S. Fitch (Ed.), Dordrecht, Reidel, 287.
- Hartman, K., Gehren, T. 1988, A&A, 199, 269.
- Heard, 1956, in Publ. David Dunlap Obs., 2,107.
- Hooten, J.T., Hall, D.S. 1990, ApJS, 74, 225.
- Jenkins, L.F. 1952 and 1963, General Catalogue of Trigonometric Stellar Parallaxes, Yale University Observatory, New Haven.

- Johnson, H.M., Mayor, M. 1986, *ApJ*, 310, 354.
- Laird, J.B., Carney, B.W., Latham, D.W. 1988, *AJ*, 95(6), 1843.
- Latham, D.W., Mazeh, T., Carney, B.W., McCrosky, R.E., Stefanik, R.P., Davis, R.J. 1988, *AJ*, 96(2), 567.
- Latham, D.W., Mazeh, T., Stefanik, R.P., Davis, R.J., Carney, B.W., Krymolowski, Y., Laird, J.B., Torres, G., Morse, J.A. 1992, *AJ*, 104(2), 774.
- Lindgren, H., Ardeberg, A. 1995, *A&A*, in press.
- Lindgren, H., Ardeberg, A., Zuiderwijk, E. 1987, *A&A*, 188, 39.
- Mayor, M., Turon, C. 1982, *A&A*, 110, 241.
- Meyer, J.P. 1985, *ApJS*, 57, 173.
- Ottmann, R., Schmitt, J.H.M.M. 1992, *A&A*, 256, 421.
- Ottmann, R. 1993, *A&A*, 273, 546.
- Pallavicini, R., Golub, L., Rosner, R., Vaiana, G.S., Ayres, T., Linsky, J.L. 1981, *ApJ*, 248, 279.
- Pasquini, L., Fleming, T., Spite, F., Spite, M. 1991, *A&A*, 249, L23.
- Pasquini, L., Lindgren, H. 1994, *A&A*, 283, 179.
- Pasquini, L., Belloni, T. 1994, in *Eighth Cambridge Workshop on Cool Stars, Stellar Systems and the Sun*, J.-P.Caillault (Ed.).
- Peterson, R., Willmarth, D.W., Carney, B.W., Chaffee, F.H. 1980, *ApJ*, 239, 928.
- Pfeffermann, E., Briel, U.G., Hippmann, H., Kettenring, G., Metzner, G., Predehl, P., Reger, G., Stephan, K.-H. 1987, MPE print, 81.
- Randich, S., Gratton, R., Pallavicini, R. 1993, *A&A*, 273, 194.
- Randich, S., Giampapa, M.S., Pallavicini, R. 1994, *A&A*, 283, 893.
- Rodono, M., Cutispoto, G., Messina, S. 1994, *A&A*, 281, 756.
- Sandage, A., Fouts, G. 1987, *AJ*, 93, 74.
- Schmitt, J.H.M.M. 1985, *ApJ*, 293, 178.
- Schmitt, J.H.M.M., Collura, A., Sciortino, S., Vaiana, G.S., Harnden, F.R., Rosner, R. 1990, *ApJ*, 365, 704.
- Schrijver, C.J., van den Oord, G.H.J., Mewe, R. 1994, *A&A*, 289, L23.
- Schrijver, C.J., Mewe, R., van den Oord, G.H.J., Kaastra, J.S. 1995, *A&A*, 302, 438.
- Singh, K.P., Drake, S.A., White, N.E. 1995, *ApJ*, 445, 840.
- Singh, K.P., White, N.E., Drake, S.A. 1996, *ApJ*, 456, 766.
- Spite, M., Pasquini, L., Spite, F. 1994, *A&A*, 290, 217.
- Stern, R.A., Lemen, J.R., Schmitt, J.H.M.M., Pye, J.P. 1995, *ApJ*, 444, L45.
- Strassmeier, K.G., Hall, D.S., Zeilik, M., Nelson, E., Eker, Z., Fekel, F.C. 1988, *A&AS*, 72, 291.
- Tanaka, K., Zirin, H. 1985, *ApJ*, 299, 1036.
- Trümper, J. 1983, *Adv. Space Res.*, 4, 241.
- Van den Berg, D., Bell, R.A. 1985, *ApJS*, 58, 561.
- Voges, W. 1995, private communication.
- Zahn, J.-P. 1977, *A&A*, 57, 383.
- Zimmermann, H.U., Becker, W., Belloni, T., Döbereiner, S., Izzo, C., Kahabka, P., Schwendtker, O. 1994, *EXSAS User's Guide*, MPE Report, 257.